Monica E. Peek, M.D., M.P.H., M.S.
University of Chicago Pritzker School of Medicine
Chicago, Illinois

Craig M. Coopersmith, M.D.
Emory University School of Medicine
Atlanta, Georgia

Kelly N. Michelson, M.D., M.P.H.
Northwestern University Fienberg School of Medicine
Chicago, Illinois

William F. Parker, M.D., M.S.‡
University of Chicago Pritzker School of Medicine
Chicago, Illinois

ORCID IDs: 0000-0002-9640-6720 (S.V.B.); 0000-0002-7434-6747 (L.N.S.-P.).

*These authors contributed equally to this work.
‡Corresponding author (e-mail: wparker@uchicago.edu).

References

1. Institute of Medicine. Crisis standards of care: a systems framework for catastrophic disaster response. Vol. 1: Introduction and CSC framework. Washington, DC: The National Academies Press; 2012 [accessed 2021 Oct 19]. Available from: https://doi.org/10.17226/13351.
2. Piscitello GM, Kapania EM, Miller WD, Rojas JC, Siegler M, Parker WF. Variation in ventilator allocation guidelines by US state during the coronavirus disease 2019 pandemic: a systematic review. *JAMA Netw Open* 2020;3:e2012606.
3. Rosenbaum L. Facing Covid-19 in Italy—ethics, logistics, and therapeutics on the epidemic's front line. *N Engl J Med* 2020;382: 1873–1875.
4. New York State Department of Health and New York State Task Force on Life and the Law Update Ventilator Allocation Guidelines; 2015 [accessed 2021 Oct 19]. Available from: https://health.ny.gov/regulations/task_force/reports_publications/docs/ventilator_guidelines.pdf
5. Daugherty Biddison EL, Faden R, Gwon HS, Mareiniss DP, Regenberg AC, Schoch-Spana M, *et al.* Too many patients … a framework to guide statewide allocation of scarce mechanical ventilation during disasters. *Chest* 2019;155:848–854.
6. Wunsch H, Hill AD, Bosch N, Adhikari NKJ, Rubenfeld G, Walkey A, *et al.* Comparison of 2 triage scoring guidelines for allocation of mechanical ventilators. *JAMA Netw Open* 2020;3:e2029250.
7. Gershengorn HB, Holt GE, Rezk A, Delgado S, Shah N, Arora A, *et al.* Assessment of disparities associated with a crisis standards of care resource allocation algorithm for patients in 2 US hospitals during the COVID-19 Pandemic. *JAMA Netw Open* 2021;4: e214149.
8. Snow GL, Bledsoe JR, Butler A, Wilson EL, Rea S, Majercik S, *et al.* Comparative evaluation of the clinical laboratory-based Intermountain risk score with the Charlson and Elixhauser comorbidity indices for mortality prediction. *PLoS One* 2020;15:e0233495.
9. White DB, Lo B. Mitigating inequities and saving lives with ICU triage during the COVID-19 pandemic. *Am J Respir Crit Care Med* 2021;203: 287–295.
10. Daniels N. Just health: meeting health needs fairly. New York: Cambridge University Press; 2007.
11. Persad G, Joffe S. Allocating scarce life-saving resources: the proper role of age. *J Med Ethics* [online ahead of print] 22 Mar 2021; DOI: 10.1136/medethics-2020-106792.
12. Antiel RM, Curlin FA, Persad G, White DB, Zhang C, Glickman A, *et al.* Should pediatric patients be prioritized when rationing life-saving treatments during COVID-19 pandemic. *Pediatrics* 2020;146: e2020012542.

Machine Learning–based Sleep Staging in Patients with Sleep Apnea Using a Single Mandibular Movement Signal

To the Editor:

We all sleep, and sleep patterns and architecture influence our health and wellbeing. At present, the gold standard method for recording detailed sleep patterns to detect and monitor sleep disorders is in-laboratory overnight polysomnography (PSG), requiring specialized equipment and trained staff. This is no longer feasible in view of the size of the population with suspected sleep disorders, and especially in the coronavirus disease (COVID-19) era (1).

Mandibular movements reveal the changes in trigeminal motor nucleus activity driven by brainstem centers involved in sleep and wake transitions (2, 3). The activity of upper airway muscles anchored on the mandibular jaw is the net result of the activation of brainstem respiratory and sleep centers and their respective interactions. This produces specific mandibular movement patterns reflecting the interactions between sleep stages and respiratory control. We previously demonstrated that sleep mandibular movements represent a powerful tool for characterizing respiratory disturbances in obstructive sleep apnea (OSA) (4–6).

Figure 1 gives examples of how the different sleep stages each have typical mandibular movement signal patterns.

Recordings of mandibular movements throughout the night provide hundreds of temporal–spatial signals for modeling and

Supported by the French National Research Agency in the framework of the "Investissements d'avenir" program (ANR-15-IDEX-02) and the "e-health and integrated care and trajectories medicine and MIAI artificial intelligence" chairs of excellence from the Grenoble Alpes University Foundation (J.-L.P., R.T., and S.B.). This work has also been partially supported by Multidisciplinary Institute in Artificial Intelligence @ Grenoble Alpes (ANR-19-P3IA-0003). The devices used in the study were provided by Sunrise, Namur, Belgium.

Author Contributions: N.-N.L.-D. conceived and designed the project, analyzed the data, drafted the initial manuscript, and reviewed and revised the manuscript; J.-B.M. conceived and designed the study, performed the research, analyzed the data, drafted the initial manuscript, and reviewed and revised the manuscript; N.C. and V.C. performed the research and participated in data acquisition; R.T. reviewed and revised the manuscript; S.B. analyzed the data and reviewed and revised the manuscript; J.-L.P. conceived and designed the study, analyzed the data, and reviewed and revised the manuscript. All authors helped revise the manuscript and approved it for submission.

Data sharing statement: The deidentified data used in this study are not publicly available at present. Parties interested in data access should contact N.-N.L.-D. (nam@hellosunrise.com) for queries related to the Extreme Gradient Boosting (XGB) classifier and J.-B.M. (martinot.j@respisom.be) for queries related to the sleep laboratory data set. The data sets generated and/or analyzed during the current study are available from the corresponding author on reasonable request. Applications will need to undergo ethical and legal approvals by the respective institutions. Those interested in research collaborations should contact J.-B.M. (martinot.j@respisom.be).

Originally Published in Press as DOI: 10.1164/rccm.202103-0680LE on July 23, 2021

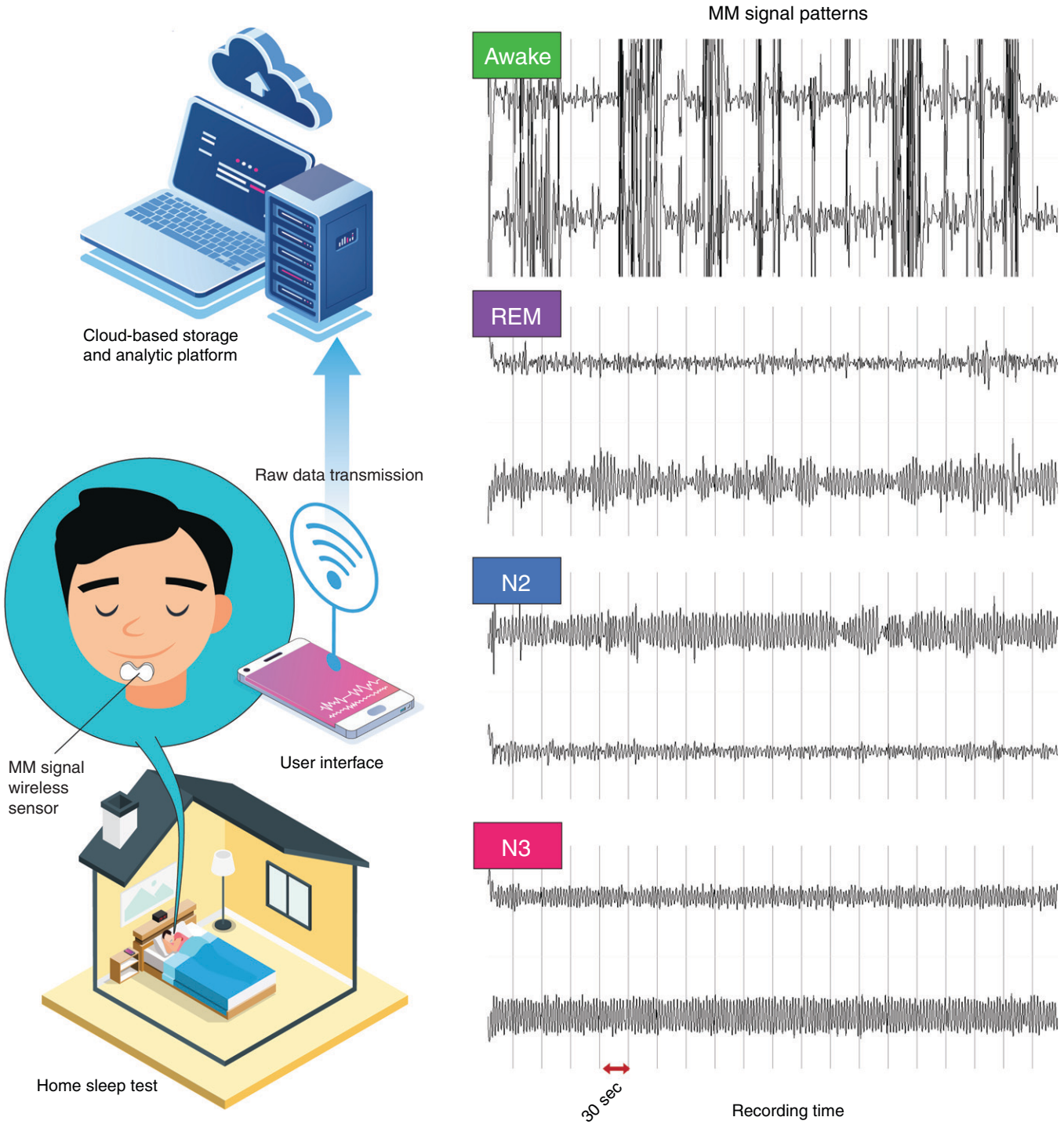

Figure 1. The mandibular movements (MM) signal processed by machine learning to provide sleep staging. Typical example of two of the six channels (upper and lower trace) of the MM signal recorded by a single sensor during the four sleep stages in a single individual. Each trace represents a 210-second (3.5-min) time span of MM recordings by the Sunrise system (inertial measurement with six channels) during wakefulness (top), REM sleep, light sleep, and deep sleep (bottom). Thirty-second epochs were used for sleep stage classification. Sleep is detected when MM occur at the breathing frequency. During light sleep (N2), the amplitude of MM reaches several tenths of a millimeter and varies slightly. The movements during quiet respiration and light sleep are repeated at a frequency ranging between 0.15 and 0.60 Hz depending on central drive output. Deepening of sleep (N3) increases the upper airway's resistance, and this is reflected by an increase in the amplitude of movement, which is also more stable than during N2. REM sleep is easily identified by irregular frequencies and changing amplitudes in MM that are on average smaller than non-REM sleep amplitudes. Cartoon images adapted from Freepik.com.

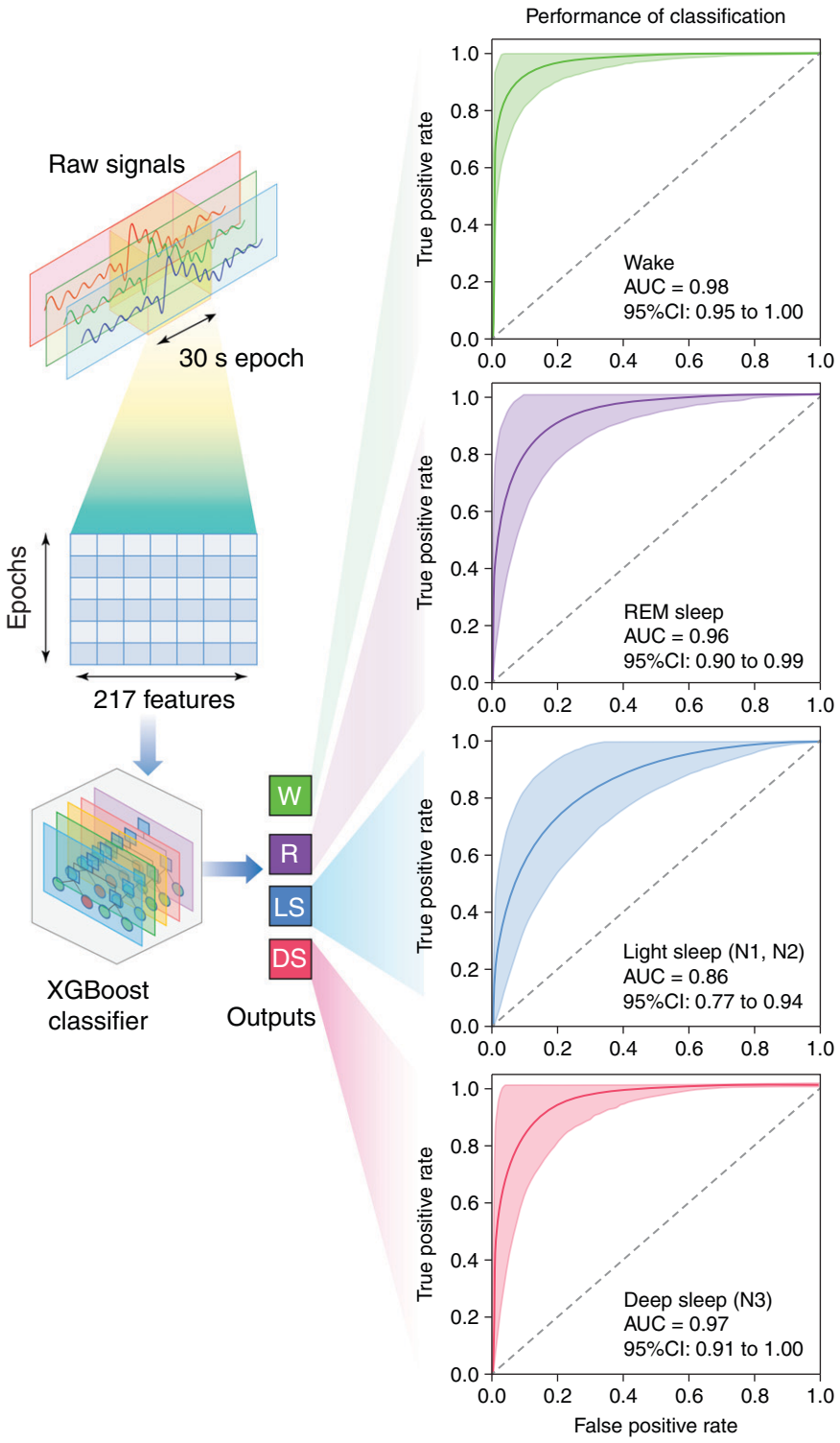

Figure 2. Stagewise receiver operating characteristics (ROC) curve analysis. This consisted of extracting prediction scores for each target stage (wake, light sleep, deep sleep, and REM sleep) and for each patient, then estimating the false and true positive rates of a binary one-versus-rest classification rule to establish the ROC curve. The 95% CIs of the area under the curve (AUC) and smoothing effect were obtained from empirical data (without using any resampling). The diagonal dashed line serves as a reference and shows the performance if sleep staging had been made randomly. The algorithm performed well in detecting REM sleep with a ROC–AUC of 0.96 (0.90–0.99) and non-REM deep sleep with a ROC–AUC of 0.97 (0.91–0.99). Only light non-REM sleep was slightly less well detected with an ROC–AUC of 0.86 (0.77–0.94).
CI = confidence interval; DS = deep sleep; LS = light sleep; R = REM sleep; W = wake.

identifying the different sleep stages. Our objective was to develop, train, and then validate an artificial intelligence algorithm to stage sleep using a single sensor detecting mandibular movements.

This prospective study included 1,026 adults with suspected OSA referred for overnight in-laboratory PSG and simultaneous recordings of mandibular movements using the Sunrise system (IRB 00004890; number B707201523388).

The PSG data (Somnoscreen Plus, Somnomedics) were manually scored by two experienced sleep technicians (interobserver agreement, 92.1%; 95% confidence interval [CI], 0.89–0.94; $P < 0.001$) in accordance with criteria of the American Academy of Sleep Medicine (7).

The Sunrise system is composed of a coin-sized sensor attached by the sleep technician to the chin of the patient (Figure 1). The embedded inertial measurement device senses mandibular movements and is externally controlled by a smartphone application via Bluetooth, automatically transferring nightly data to a cloud-based infrastructure (2).

Using the Extreme Gradient Boosting classifier as the core algorithm, we developed and progressively trained a machine learning sleep staging algorithm (8) using the overnight PSG and mandibular movement recordings from 800 of the patients. The algorithm automatically classified each 30-second epoch of mandibular movement patterns as wake, light non-REM (NREM; N1 + N2), deep NREM (N3), or REM sleep stage (Figure 1). N1 and N2 stages were combined in the automated scoring to reach the best compromise between clinical relevance and best model performances. The extracted features consisted of a combination of raw signals along the three axes of the accelerometer/gyroscope, processing modes (filters with different frequency bands, moving average), and statistical functions. The statistics applied to the above features were tendency toward centrality (mean, median), extreme values (min, max), quartiles, and SD, as well as the normal standardized version of all above features. The programming language was Python.

Patients in the machine learning training set ($n = 800$ [451 males]) were aged 48.4 years (16.7) with a body mass index [BMI] of 29.1 kg/m^2 (10.2), and neck circumference of 40.0 cm (5.0), all median (interquartile range [IQR]) respectively. PSG recordings showed apnea–hypopnea, respiratory disturbance, and microarousal indexes of 17.1 (27.5), 23.9 (28.5), and 24.2 (20.2), all median events/hour (IQR); and PSG sleep parameters: total sleep time 372 minutes (122.7), sleep efficiency 85.1% (13.7), and wake time 12.2% (16.5), all median (IQR).

Patients in a separate validation set ($n = 226$ [116 males]) had similar characteristics: 46.5 years (17.5), a BMI of 32.3 kg/m^2 (11.5), and neck circumference of 40.0 cm (5.0), all median (IQR); similar PSG indexes (20.3 [23.5], 27.0 [23.6], and 25.0 [20.3] for apnea–hypopnea, respiratory disturbance, and microarousal, all median [IQR] respectively), and sleep parameters: 397 min (95.7), 87.1% (11.8), and 11.5% (12.2), all median (IQR) for total sleep time, sleep efficiency, and wake time, respectively.

In the validation set, quantitative agreement analysis between machine learning and human scorings was estimated using a linear mixed model by a two-way intraclass correlation coefficient (ICC) (A, 1) (95% CI) for total sleep time, wake time, light NREM, deep NREM, and REM sleep stages: 0.94 (0.93–0.96), 0.90 (0.88–0.92), 0.70 (0.63–0.76), 0.66 (0.58–0.73), and 0.65 (0.56–0.72), respectively. The mean (95% CI) measurement bias for total sleep time and the four sleep stages (as above) were −13.0 minutes (−52.9 to +19.0), +3.8% (−6.8 to +16.8), −14.9% (−31.1 to +1.8), +6.0% (−6.0 to +21.2), and +8.4 (−21.3 to +2.4).

The algorithm classified sleep epochs with substantial qualitative agreement with manual PSG scorers, which improved as the size of the learning set was progressively increased ($\kappa = 0.71$ and accuracy = 78.3% using the full machine learning data set of 800 patients). As shown in Figure 2, a sleep stagewise receiver operating characteristics curve analysis confirmed the well-balanced performance for each target sleep stage.

Wakefulness was clearly discriminated from sleep states with a sensitivity of 88% (95% CI, 71–99%) and a specificity of 94% (85–98%). Moreover, the algorithm performed well in detecting REM sleep (sensitivity 83% [64–97%], specificity 89% [76–97%]) and deep sleep (sensitivity 84% [59–100%], specificity 90% [79–98%]). Light NREM sleep was slightly less well detected (sensitivity 60% [36–82%], specificity 88% [79–96%]).

These findings indicate that machine learning analysis of mandibular movements identifies sleep stages with good agreement to that of individual manual scorers of PSG data.

A strength of this work is that it was conducted using a real-life cohort consisting of both subjects for whom PSG detected no OSA and patients with a broad spectrum of OSA, who were randomly sampled into training and validation sets.

Clear advantages of our approach are that it relies on a highly performant sleep staging algorithm processing signals from a single mandibular movement, facilitating the complex process of signal treatment and improving sleep staging reproducibility.

Our study was designed to avoid the limitations occurring in other studies. First, PSG sleep staging was performed by two experienced technicians. Second, data from an independent set of patients were used to validate the algorithm. The input data were balanced using a random resampling (SMOTE) technique to minimize the effect of data imbalance. A conventional algorithmic framework implying manual feature extraction and a structured data-driven algorithm was adopted for better control and understanding of input data. Furthermore, the XGBoost algorithm offers several advantages over classical methods, including high efficiency in computation and resources, allowing for fast training and execution speed.

In conclusion, the mandibular movement signal acquired from a compact inertial measurement device is suitable for automated sleep staging in adults presenting a broad spectrum of OSA severity. The proposed algorithm performs well for clinical applications and could present a major step forward toward unobtrusive, reliable, and cost-effective home-based sleep assessment and value-based care (9). ■

Author disclosures are available with the text of this letter at www.atsjournals.org.

Acknowledgment: The authors thank Ravzat Ashurlaeva (Respisom, Erpent, Belgium), who kindly spent innumerable hours providing secretarial assistance, and Alison Foote, Ph.D. (Grenoble Alpes University Hospital, France), for critical reading and substantial editing of the letter.

Nhat-Nam Le-Dong, M.D., Ph.D.*
Sunrise
Namur, Belgium

Jean-Benoit Martinot, M.D.*‡
Centre Hospitalier Universitaire - Université Catholique de Louvain Namur Site Sainte-Elisabeth
Namur, Belgium

and

Université Catholique de Louvain Bruxelles Woluwe
Brussels, Belgium

Nathalie Coumans, M.Sc.
Valérie Cuthbert, M.Sc.
Centre Hospitalier Universitaire - Université Catholique de Louvain Namur Site Sainte-Elisabeth
Namur, Belgium

Renaud Tamisier, M.D., Ph.D.
Sébastien Bailly, Pharm.D., Ph.D.
Jean-Louis Pépin, M.D., Ph.D.
University Grenoble Alpes
Grenoble, France

and

Grenoble Alpes University Hospital
Grenoble, France

ORCID ID: 0000-0001-8536-7300 (J.-B.M.).

*Co–first authors.
‡Corresponding author (e-mail: martinot.j@respisom.be).

References

1. Benjafield AV, Ayas NT, Eastwood PR, Heinzer R, Ip MSM, Morrell MJ, *et al.* Estimation of the global prevalence and burden of obstructive sleep apnoea: a literature-based analysis. *Lancet Respir Med* 2019;7: 687–698.
2. Kubin L. Neural control of the upper airway: respiratory and state-dependent mechanisms. *Compr Physiol* 2016;6: 1801–1850.
3. Moore JD, Kleinfeld D, Wang F. How the brainstem controls orofacial behaviors comprised of rhythmic actions. *Trends Neurosci* 2014;37: 370–380.
4. Pépin JL, Letesson C, Le-Dong NN, Dedave A, Denison S, Cuthbert V, *et al.* Assessment of mandibular movement monitoring with machine learning analysis for the diagnosis of obstructive sleep apnea. *JAMA Netw Open* 2020;3:e1919657.
5. Martinot JB, Borel JC, Cuthbert V, Guénard HJP, Denison S, Silkoff PE, *et al.* Mandibular position and movements: Suitability for diagnosis of sleep apnoea. *Respirology* 2017;22:567–574.
6. Martinot JB, Le-Dong NN, Cuthbert V, Denison S, Silkoff PE, Guénard H, *et al.* Mandibular movements as accurate reporters of respiratory effort during sleep: validation against diaphragmatic electromyography. *Front Neurol* 2017;8:353.
7. Berry RB, Brooks R, Gamaldo C, Harding SM, Lloyd RM, Quan SF, *et al.* AASM Scoring Manual updates for 2017 (version 2.4). *J Clin Sleep Med* 2017;13:665–666.
8. Chen T, Guestrin C. XGBoost: a scalable tree boosting system. 22nd SIGKDD Conference on Knowledge Discovery and Data Mining 2016; 785–794.
9. Pépin JL, Baillieul S, Tamisier R. Reshaping sleep apnea care: time for value-based strategies. *Ann Am Thorac Soc* 2019;16: 1501–1503.

Check for updates

Elexacaftor/Tezacaftor/Ivacaftor Improved Clinical Outcomes in a Patient with N1303K-CFTR Based on *In Vitro* Experimental Evidence

To the Editor:

The new generation of *CFTR* (cystic fibrosis transmembrane conductance regulator) protein modulator, the triple combination consisting of elexacaftor/tezacaftor/ivacaftor (ETI), has been recognized as highly effective therapy for patients 12 years or older with cystic fibrosis (CF) and at least one F508del-CFTR allele. Recently, ETI has also shown clinically meaningful benefits both in patients with CF with advanced lung disease (baseline $\%FEV_1 < 40$) (1–3) and in children 6 through 11 years with CF and at least one F508del allele (4). Similar results from different institutions have also been reported in conference abstracts (5–7). However, it is unclear if ETI is therapeutically beneficial to patients with CF with N1303K, another class II CFTR mutant. Using the whole-cell patch-clamp recording and biochemical approaches, we demonstrated that ETI increased maturation and function of N1303K-CFTR. After *in vitro* confirmation, we investigated if ETI would be beneficial to a patient with CF with two non-F508del-CFTR mutations, N1303K and E193X, and our findings are reported below.

Methods

To monitor CFTR function, HEK293 cells were transiently transfected with indicated CFTR variants. Cotransfection of GFP-expression plasmid was performed for positive selection. Cells were treated with 2 μM VX445/VX661 (elexacaftor/tezacaftor, MedChemExpress) for about 24 hours after overnight transfection. Whole-cell patch-clamp recordings were performed using an Axopatch-200B amplifier connected to Axon DigiData 1550B (Molecular Devices). Patch pipettes were prepared using a micropipette puller (P-1000; Sutter Instrument). To simultaneously obtain current traces at −60 mV and *I*/*V* curves of CFTR, whole-cell currents were consecutively recorded with a 1 s voltage ramp of ±100 mV applied every 10 s: hold at Vm (membrane voltage) = −60 mV and filtered at 1 kHz and sampled at 50 Hz. The pipette solution containing VX770 (ivacaftor, 2 μM, SelleckChem) was composed of (in mM) 116 *N*-methyl-D-glucamine chloride ($NMDG\text{-}Cl^-$), 30 aspartic acid, 1 $MgCl_2$, 5 ethyleneglycol-*bis*-(β-aminoethyl ether)-*N,N,N′,N′*-tetraacetic acid, 2.9 $CaCl_2$, 10 *N*-2-hydroxyethylpiperazine-*N′*-ethane sulfonic acid, and 3 MgATP, pH 7.4. Bath solution was composed of (in mM): 146 $NMDG\text{-}Cl^-$, 1 $CaCl_2$, 1 $MgCl_2$, 10

Supported by funding from the NHLBI and the National Institute of Diabetes and Digestive and Kidney Diseases (DK093045, DK080834, HL147351, P30-DK117467) and from Cystic Fibrosis Foundation (Postdoc-to-Faculty Transition Award, HUANG20F5 and CFF-RDP NAREN19R0).

Author Contributions: Designed and performed experiments: Y.H., G.P., J.L., S.Y., and K.M.; analyzed data and drafting the manuscript: Y.H., G.P., J.L., and A.P.N.; conception and design: A.P.N. All authors read the manuscript and approved the final version.

Originally Published in Press as DOI: 10.1164/rccm.202101-0090LE on August 11, 2021